Int J Adv Manuf Technol (2015) 77:1935–1941
DOI 10.1007/s00170-014-6579-8

ORIGINAL ARTICLE

Enhanced grinding performance by means of patterned grinding wheels

Berend Denkena · Thilo Grove · Tim Göttsching · Eraldo Jannone da Silva · Reginaldo Teixeira Coelho · Remo Filleti

Received: 28 July 2014 / Accepted: 9 November 2014 / Published online: 23 November 2014

Abstract In this paper, a new and innovative method for the patterning of grinding wheels is presented. The patterns are machined with a patterning tool by using fly-cutting kinematics. By changing the patterning process parameters, different pattern sizes and densities can be machined in a flexible way. Surface and cylindrical grinding experiments show that grinding with patterned grinding wheels can significantly reduce process forces, grinding burn, and grinding power. The surface roughness increases because less active cutting edges remain when grinding with patterned wheels. But especially for roughing processes, the results show great potential for increasing the overall grinding performance.

Keywords Grinding · Grinding performance · Patterning · Fly-cutting

1 Introduction

Grinding is an important manufacturing process, especially if high surface qualities have to be realized or if hard or brittle materials have to be machined [1]. Nevertheless, the productivity of grinding processes is often limited due to workpiece failure, caused by a high thermal load in the contact zone. When grinding with vitrified bonded aluminum oxide grinding wheels, up to 75 % of the mechanical energy is converted into heat that diffuses directly into the workpiece [2]. Therefore, in recent years, many research activities have focused on the reduction of the thermal load in the contact zone by applying new innovative grinding tools with a modified grinding wheel topography. The topographies of these tools are intermitted. This can be realized by using specially manufactured grinding wheels with a segmented abrasive coating or with a defined grain pattern [3–6]. Other researchers have developed a special dressing method to generate a reduced effective contact area or have applied laser techniques for machining voids into the coating [7, 8]. In summary, most of the concepts require non-standard grinding tools or a cost-intensive manufacturing process, such as laser technology for creating a patterned grinding wheel topography. Given that today's manufacturing processes have to be highly flexible in order to machine customized parts with a large geometrical variety, the introduced concepts do not meet these requirements [9]. Therefore, an innovative method for machining patterns into the grinding wheel topography in a flexible and productive way was developed by Denkena et al. [10] by using a fly-cutting kinematic and a standard dressing spindle.

Parallel the use of patterned grinding wheels has been investigated for the manufacturing of textured surfaces. But those patterned wheels have not been used for productivity enhancement [11, 12]. Here, a flexible method for creating a patterned grinding wheel was designed by Oliveira et al. [13] by employing a controlled shaker for dressing. The aim of those investigations is the generation of tribological optimized surfaces for friction reduction by means of face or cylindrical grinding. Patterns or microdimples are transferred from the grinding wheel topography to the workpiece. Those patterns or dimples increase the fluid retention capacity of a sliding system and therefore reduce the overall friction [14].

B. Denkena · T. Grove · T. Göttsching (✉)
Institute of Production Engineering and Machine Tools, Leibniz Universität Hannover, An der Universität 2, 30823 Garbsen, Germany
e-mail: goettsching@ifw.uni-hannover.de

E. J. da Silva (✉) · R. T. Coelho · R. Filleti
Laboratory of Advanced Processes and Sustainability, Universidade de São Paulo, Av. Trabalhador Sao-carlense, 400, 13566-590 Sao Carlos, Brazil
e-mail: eraldojs@sc.usp.br

Nevertheless, only few research activities have focused on using those grinding wheels for enhancing the grinding performance [13].

In this paper, the patterning of vitrified bonded grinding wheels by applying a fly-cutting kinematic for enhancing the overall grinding performance will be presented. In contrast to the results of other researchers, comparatively small patterns will be machined into the grinding wheel surface. Face grinding and cylindrical grinding experiments will be conducted in order to analyze the overall potential of enhancing the grinding performance by means of patterning. Finally, possible future industrial applications for each process will be identified.

2 Patterning with fly-cutting kinematic

The developed patterning process for grinding wheels can be integrated into any conventional grinding machine by using a common dressing spindle equipped with a patterning tool. This tool is a specially manufactured disc with single diamonds placed along the circumference. The patterning process is graphically illustrated in Fig. 1. For the experiments presented in this paper, two different patterning tools with one and four diamonds were used. The patterning tool is connected with a common dressing spindle and placed beneath the grinding wheel such as a standard form roller. By adjusting the speed of grinding wheel and patterning tool (v_s and v_{tool}), as well as the depth of patterning cut (a_{ed}) and feed rate (v_f), the patterning can be conducted. Due to the discontinuous machining of just a single cutting edge and the overlapping of two moving directions, single patterns appear on the grinding wheel topography.

The pattern length (l_{pat}) (Fig. 2) is primarily influenced by the tool radii (r_s and r_{tool}) as well as the relative speed between grinding wheel and cutting tool. According to Grün [15], the pattern length is calculated as follows:

$$l_{pat} = \sqrt{2*r_s^2*(1-\cos(\alpha_s))} \tag{1}$$

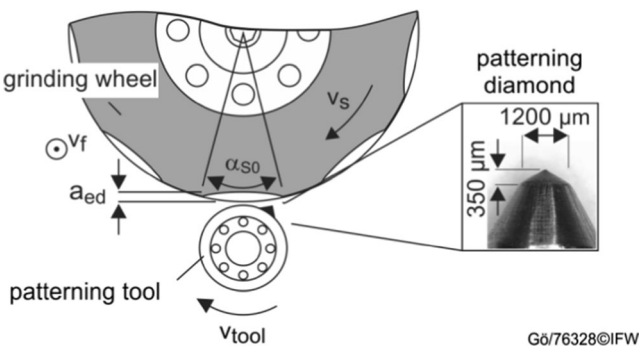

Fig. 1 Schematic representation of the patterning process

with the resulting angle α_S, which is the engagement angle α_{S0} between patterning tool and grinding wheel multiplied with the relative speed. The positive and negative sign indicate the patterning tool speed direction regarding the grinding wheel speed (+: counterclockwise, −: clockwise):

$$\alpha_s = \left(1 \pm \frac{n_s}{n_{tool}} * \frac{r_s}{r_{tool}}\right) * \alpha_{s0} \tag{2}$$

The engagement angle α_{S0} is derived from the contact conditions by using trigonometry:

$$\alpha_{s0} = 2*\arccos\frac{(r_s + r_{tool} - a_e)^2 + (r_s)^2 - r_{tool}^2}{2*(r_s + r_{tool} - a_e)*(r_s)} \tag{3}$$

Another process parameter influencing the pattern length (l_{pat}) is the patterning depth (a_{pat}), which is identical with the depth of cut (a_{ed}). An increased depth leads to a larger pattern width (b_{pat}) due to the conical tool profile as well as to a longer contact length between tool and grinding wheel. The patterns having a length of about l_{pat}=3–7 mm and a width of b_{pat}= 0.2–0.5 mm are machined with a depth of a_{pat}=20–100 µm. The spacing between the patterns in axial direction (s_{ax}) is identical with the feed rate (f) during patterning and can be adjusted by the numerical control. The pattern size and arrangement is a function of the process parameters described in Fig. 2. The number of patterns created by one single turn of the grinding wheel depends on the frequency ratio (λ) between grinding wheel rotational frequency (n_s) and tool rotational frequency (n_{tool}) as well as the number of diamonds (n_{diam}). The spacing of the patterns along the grinding wheel circumference (s_{tan}) can be derived from this ratio.

The tool trajectories of a single grinding wheel revolution are schematically illustrated in Fig. 3 for up-patterning mode and a frequency ratio of 8 and 32, respectively. With an increasing frequency ratio (λ), the patterns get shorter due to a decreased effective cutting time. The area of the grinding wheel between the patterns is called effective contact area (A_{eff}), as this area will be in direct contact with the workpiece

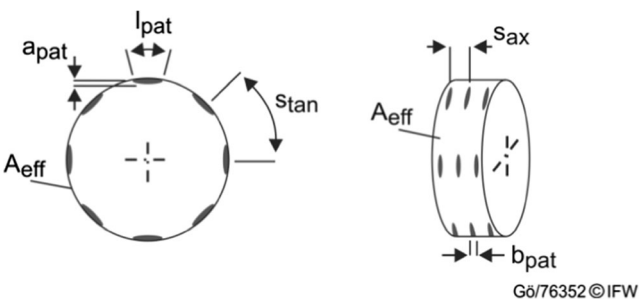

Fig. 2 Characteristic geometrical parameters of the patterning process

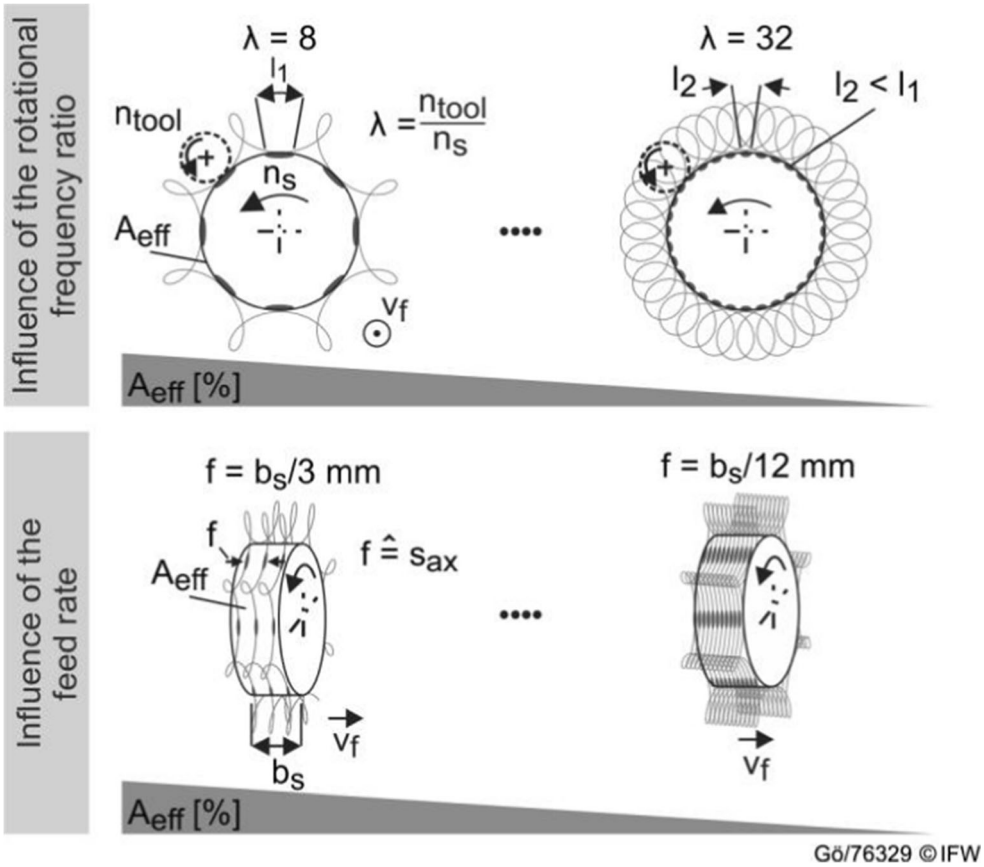

Fig. 3 Effective contact area of a patterned grinding wheel

while grinding. With an increased frequency ratio (λ), the effective contact area decreases. Similar behavior occurs if the tangential feed motion (v_f) during the patterning process is minimized. More tool trajectories repeat itself with a defined offset between each other and therefore increase the pattern density.

The grinding wheels used for this research have a diameter of d=300 mm for face grinding and d=400 mm for cylindrical grinding. In order to pattern the whole circumference of such grinding wheels with a patterning tool with only one cutting edge (n_{diam}=1), high patterning spindle frequencies or extremely low grinding wheel frequencies are required. The grinding machines used in this research rotate with a minimum frequency of about 165 min^{-1}. In order to generate highly structured grinding wheel topographies, frequency ratios of λ>100 are necessary, which requires patterning spindle frequencies of up to 20,000 min^{-1}. Increasing the number of cutting diamonds enables the use of conventional dressing spindles with lower rotational speed, since the same amount of patterns can be machined with smaller frequency ratios (λ). Nevertheless, the pattern length (l_{pat}) is a function of λ (see Fig. 4). When patterning with one cutting edge (n_{diam}=1), 128 patterns are machined with a length of about 4.7 mm (λ_A=128). The feed motion stays constant resulting into an effective contact area of A_{eff}=75 %. This effective contact area slightly changes to A_{eff}=73 %, when patterning with four diamonds since the pattern length increases to l_{pat}=5 mm (λ_B=32). In order to obtain a constant effective contact area, fewer patterns have to be machined by marginally decreasing the frequency ratio (λ) or increasing the feed motion (v_f). Within this research, a patterning tool with one diamond (n_{diam}=1) has been used for the face grinding experiments and a tool equipped with four diamonds for the cylindrical grinding experiments.

3 Materials and methods

Acoustic mapping was used for process monitoring and control. The map represents the acoustic emission (AE) distribution around the grinding wheel along the time axis, according to the method proposed by Oliveira et al. [16] and Oliveira and Dornfeld [17]. The technique allows the monitoring of the contact between the wheel and the patterning tool during the patterning process in real-time. The pattern arrangement on the grinding wheel topography can be derived from the AE-signals and the proposed method by Oliveira.

In order to investigate the potential of patterned grinding wheels, two different grinding processes were used. The surface grinding experiments were conducted at the Institute of

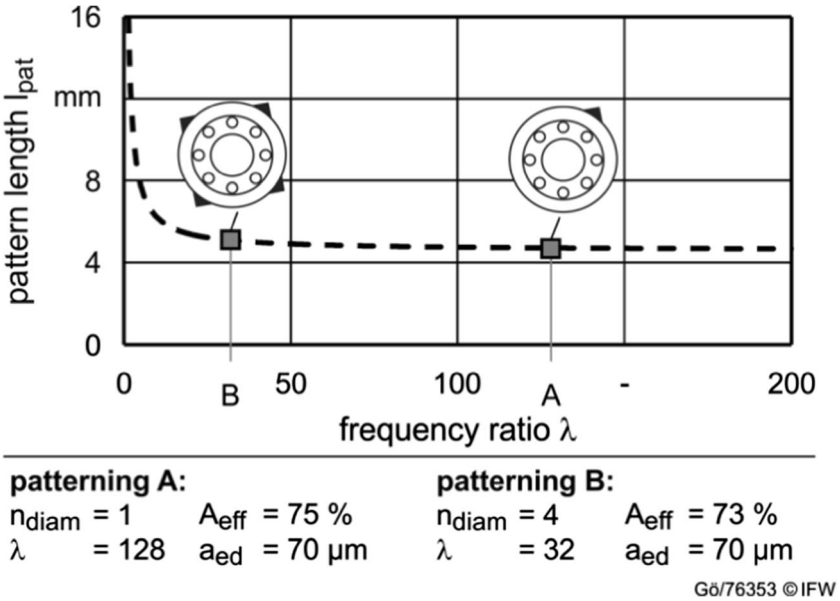

Fig. 4 Pattern length as a function of the frequency ratio for the counterclockwise patterning mode

Production Engineering and Machine Tools (IFW) in Germany on a Blohm Profimat 307 grinding machine. Then, the patterning equipment was transferred to the Laboratory of Advanced Processes and Sustainability (LAPRAS) in Brazil and installed in a Zema cylindrical grinding machine. For both tests, vitrified bonded aluminum oxide grinding wheels with a grain size of 80 mesh have been used. The workpiece material was a hardened tool steel X155CrVMo12 (1.2379) for the

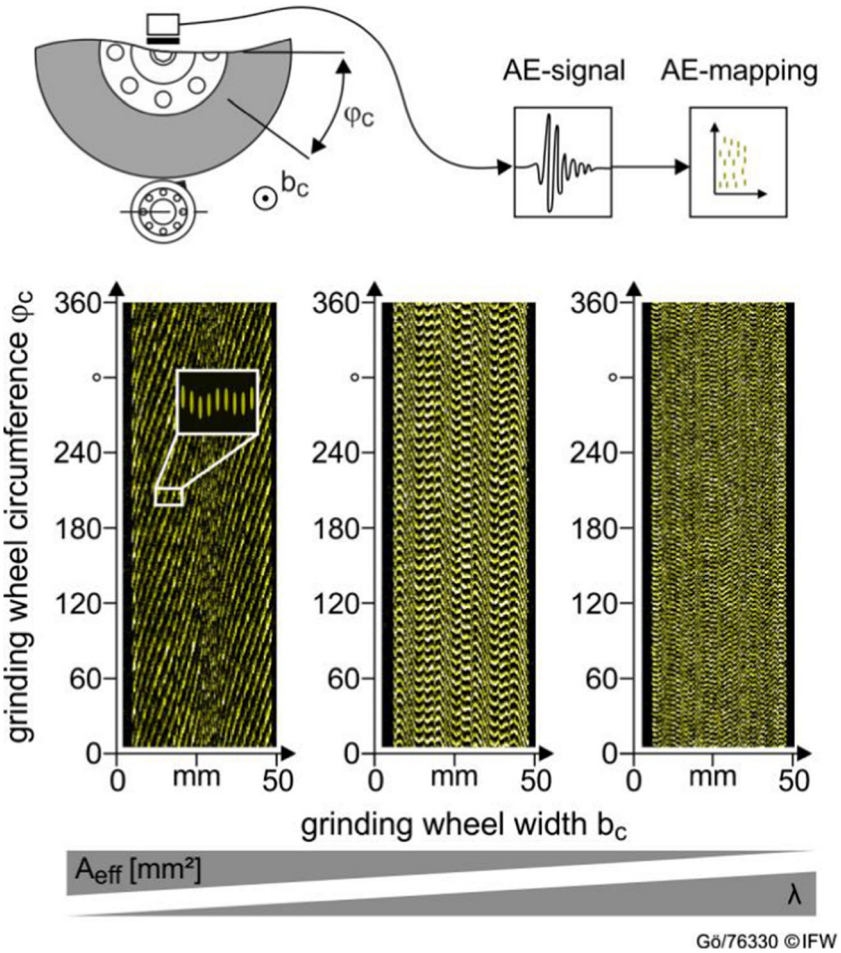

Fig. 5 AE-mapping for patterning process monitoring

surface grinding and a steel 42CrMo4 (1.7225) for the cylindrical grinding. Effective contact areas of the grinding wheel of 90 and 75 % have been realized by using a patterning tool with one diamond or rather four diamonds. Before each experiment, all grinding wheels have been dressed in an identical way. For the surface grinding experiments, a surface plate was used. The dressing parameters were set to a_{ed}=5 μm and U_d=8. The dressing process before the cylindrical grinding experiments was also conducted with a surface plate with a_{ed}=10 μm and U_d=8.

4 AE-mapping during patterning

In this chapter, the acoustic mapping method will be applied to the patterning process. In Fig. 5, the AE-mappings of three different patterning processes with λ=5, 11, and 22 using a tool with four diamonds are displayed. The contact between tool tip and grinding wheel during patterning is visualized by a bright and yellow pixel. Each pattern consists of several pixels. The patterns are aligned very close to each other along the grinding wheel width b_c, therefore they appear as a curved yellow line. Minor changes of the grinding wheel or tool spindle rotational frequency directly affect the position of a single pattern on the grinding wheel and therefore create a sinuous and not a straight pattern arrangement. In contrast to the bright pixels, the dark area is the un-machined topography of the grinding wheel, which is the effective contact area (A_{eff}) described in Fig. 3. The effective contact area (dark area) considerably decreases when λ rises because more patterns are machined along the grinding wheel circumference.

5 Influence of patterned grinding wheels in grinding

In this chapter, the results of face grinding experiments are presented. In order to prove if the results obtained by face grinding can be transferred to another grinding process

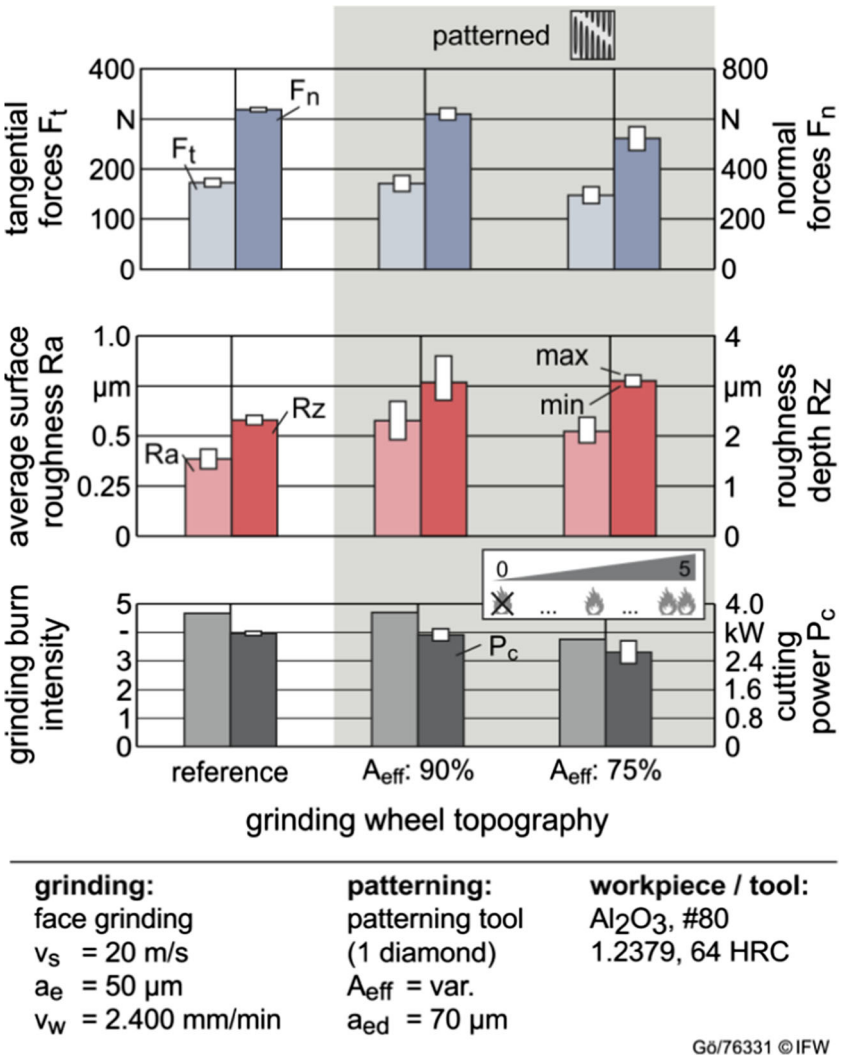

Fig. 6 Results of face grinding experiments

kinematic, cylindrical grinding experiments are conducted. The grinding results of the patterned tools are compared to the results when grinding with a non-patterned grinding wheel (reference).

5.1 Face grinding results

The results of the face grinding experiments are illustrated in Fig. 6. The process parameters were kept constant at a cutting speed of v_s=20 m/s, a feed rate of v_w=2.400 mm/min, and cutting depth of a_e=50 µm. The results show the mean value of three experimental runs.

The process forces in normal and tangential direction decrease significantly if the number of pattern rises and the effective contact area decreases to A_{eff}=75 %. Less active grains are involved in the grinding process and therefore ploughing and rubbing processes are suppressed for the benefit of a more effective cutting process due to increased microcutting in the contact zone. By reducing the number of cutting edges, the surface roughness after grinding with patterned grinding wheels is higher compared to the reference, since less kinematic overlappings of cutting paths that even the workpiece surface occur. As a result of reduced tangential forces, also less cutting power (P_c) was necessary when grinding with an effective contact area of A_{eff}=75 %. The cutting power was calculated according to:

$$P_c = F_t * v_s \tag{4}$$

After grinding, the workpiece surface was optically analyzed, and grinding burn marks have been correlated with a grinding burn intensity on a scale from 0 to 5 (0=no burning, 5=severe burning). The patterns on the grinding wheel increase the coolant flow and chip transport capacity through the contact zone and therefore reduce the thermal load. Thus, less grinding burn was detected when grinding with patterned grinding wheels.

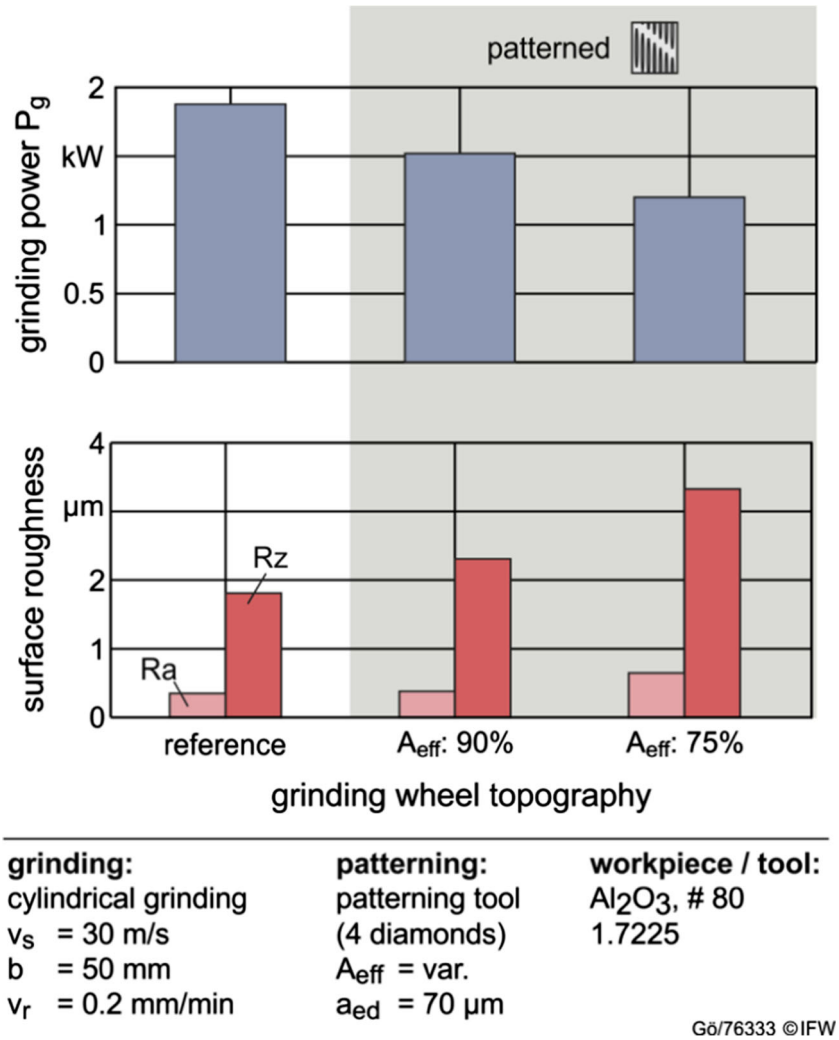

Fig. 7 Results of cylindrical grinding experiments

5.2 Cylindrical grinding results

The results of the cylindrical grinding experiments are shown in Fig. 7. The cutting velocity was v_s=30 m/s, the radial feed rate was v_{fr}=0.2 mm/min, the grinding width of cut was b= 50 mm, and a material removal rate of Q'_w=0.5 mm^3/mm*s. The spark out time was set to 2 s. Different from the face grinding experiments, the grinding power was estimated based on the net power consumption of the wheel head motor during grinding. Similar to the face grinding force results, the grinding power decreases significantly when the number of pattern is increased (lower value of effective contact area) due to the reduced contact area and increased number of patterning grooves. The grinding power was reduced from 1.9 to 1.3 kW by more than 30 %. Less power is necessary for the material removal, since the rubbing component is reduced along with the lower wheel contact area. The surface roughness values were also influenced by the changes on the effective contact area due to patterning. For the baseline condition, regular dressed wheel, with no patterning, the obtained values were *R*a=0.35 μm and *R*z=1.81 μm. When grinding with a highly patterned grinding wheel with A_{eff}=75 %, the roughness increased to *R*a=0.65 μm and *R*z=3.33 μm, due to the reduced contact area and also the additional wheel macroeffect of patterning with shallow grooves.

6 Conclusion

In this paper, a new and innovative method for the patterning of grinding wheels was presented. The patterns are machined with a patterning tool with one or four diamonds that is connected to a conventional dressing spindle. Therefore, this compact setup can be transferred to almost any grinding machine. By changing the patterning process parameters, different pattern sizes and densities resulting in different effective contact areas (A_{eff}) can be machined in a flexible way.

In order to identify the potential of patterned grinding wheels, surface and cylindrical grinding experiments have been conducted. The results show that patterned grinding wheels decrease:

- Process forces of up to 20 %
- Thermal damage in terms of grinding burn significantly
- The grinding power by over 30 %

compared to non-patterned grinding wheels. Nevertheless, this benefit goes along with an increase of the surface roughness due to less active kinematic cutting edges. Especially for roughing processes, the results show great potential for increasing the overall grinding performance, since high surface qualities are generally achieved by subsequent finishing processes. Possible future industrial applications should focus on highly thermal stressed grinding processes, such as creep feed grinding of superalloys, profile grinding of gears, or plunge grinding of crankshafts. An advantage of this patterning method is that only certain areas of the grinding wheel can be patterned to partially reduce the grinding burn for example. Therefore, process strategies need to be developed that enable the patterning of profiled grinding tools and which allow a re-patterning in order to continuously compensate grinding wheel wear.

Acknowledgments The presented investigations were undertaken with support of the German Research Foundation (DFG) and the São Paulo Research Foundation (FAPESP) within the joint project "Enhanced Grinding Performance by Means of Microdressed Grinding Wheels" (DE447/97-1).

References

1. Tönshoff, H., Denkena, B. (2013) Basics of cutting and abrasive processes. Lecture Notes in Production Engineering. Springer
2. Noyen, M. (2008) Analyse der mechanischen Belastungsverteilung in der Kontaktzone beim Längs-Umfangs-Planschleifen. Dr.-Ing. dissertation, Universität Dortmund
3. Herzenstiel P, Aurich JC (2010) CBN-grinding wheel with a defined grain pattern—extensive numerical and experimental studies. Mach Sci Technol 14:301–322
4. Uhlmann, E., Mewis J., Hochschild, L. (2010) Analyse von Schleifprozessen mit genuteten Schleifscheiben – Gegenüberstellung experimenteller und simulativer Untersuchungen. wt Werkstatttechnik online 100/6:494 – 501
5. Uhlmann E, Hochschild L (2013) Tool optimization for high speed grinding. Prod Eng Res Dev 7(2–3):185–193
6. Nguyen T, Zhang LC (2009) Performance of a new segmented grinding wheel system. Int J Mach Tools Manuf 49:291–296
7. Tawakoli T, Westkämper E, Rabiey M (2007) Dry grinding by special conditioning. Int J Adv Manuf Technol 33:419–424
8. Tawakoli T (2010) T-Dress, Optimierung der Abrichtprozesse durch innovative Abrichtrolle mit Punktkontakt. dihw Mag 3(2010):34–42
9. Müller, N. (2001) Ermittlung des Einsatzverhaltens von Sol-Gel-Korund Schleifscheiben, Dr.-Ing. dissertation RWTH Aachen
10. Denkena, B, Köhler, J., Göttsching, T. (2013) Influence of micro patterned grinding wheels on the work piece quality. Proceedings of the 13th euspen International Conference, May 2013, Berlin, 249–252
11. Da Silva E, Oliveira J, Salles B, Cardoso R, Reis V (2013) Strategies for production of parts textured by grinding using patterned wheels. CIRP Ann Manuf Technol 62(1):355–358
12. Stepien P (2009) Regular surface texture generated by special grinding process. J Manuf Sci Eng 131:011015-1–011015-7
13. Oliveira J, Bottene A, Franca T (2010) A novel dressing technique for texturing of ground surfaces. CIRP Ann Manuf Technol 59(1):361–364
14. Denkena B, Köhler J, Kästner J, Göttsching T, Dinkelacker F, Ulmer H (2013) Efficient machining of microdimples for friction reduction. J Micro Nano-Manuf 1:011003-1–011003-8
15. Grün, F. (1988) Kinematische und technologische Grundlagen des Fräsabrichtens, Fortschritts-Bericht VDI Reihe Nr. 152, VDI-Verlag, Kaiserslautern
16. Oliveira J, Dornfeld D, Winter B (1994) Dimensional characterization of grinding wheel through acoustic emission. Ann CIRP 43(1): 291–294
17. Oliveira J, Dornfeld D (2001) Application of AE contact sensing in reliable grinding monitoring. Ann CIRP 50(1):217–220